Spectral collocation for multiparameter eigenvalue problems arising from separable boundary value problems

Bor Plestenjak[a], Călin I. Gheorghiu[b], Michiel E. Hochstenbach[c]

[a] *IMFM and Department of Mathematics, University of Ljubljana, Jadranska 19, SI-1000 Ljubljana, Slovenia*
[b] *Romanian Academy, "T. Popoviciu" Institute of Numerical Analysis, PO Box 68, 400110 Cluj-Napoca 1, Romania*
[c] *Department of Mathematics and Computer Science, TU Eindhoven, PO Box 513, 5600 MB Eindhoven, The Netherlands.*
This author was supported by an NWO Vidi research grant.

Abstract

In numerous science and engineering applications a partial differential equation has to be solved on some fairly regular domain that allows the use of the method of separation of variables. In several orthogonal coordinate systems separation of variables applied to the Helmholtz, Laplace, or Schrödinger equation leads to a multiparameter eigenvalue problem (MEP); important cases include Mathieu's system, Lamé's system, and a system of spheroidal wave functions. Although multiparameter approaches are exploited occasionally to solve such equations numerically, MEPs remain less well known, and the variety of available numerical methods is not wide. The classical approach of discretizing the equations using standard finite differences leads to algebraic MEPs with large matrices, which are difficult to solve efficiently.

The aim of this paper is to change this perspective. We show that by combining spectral collocation methods and new efficient numerical methods for algebraic MEPs it is possible to solve such problems both very efficiently and accurately. We improve on several previous results available in the literature, and also present a MATLAB toolbox for solving a wide range of problems.

Keywords: Helmholtz equation, Schrödinger equation, separation of variables, Mathieu's system, Lamé's system, spectral methods, Chebyshev collocation, Laguerre collocation, multiparameter eigenvalue problem, two-parameter eigenvalue problem, three-parameter eigenvalue problem, Sylvester equation, Bartels–Stewart method, subspace methods.

1. Introduction

When we apply separation of variables to the Helmholtz equation of an elliptic membrane, we get Mathieu's system. This two-parameter eigenvalue problem (2EP) is often used as a motivation for the introduction of multiparameter eigenvalue problems (MEPs), see, e.g., [41]. Yet, it was not until [16] that this approach was actually used to compute the eigenfrequencies of an elliptic membrane. In [16] it is shown that the two-parameter approach has certain advantages with respect to the accuracy as well as to the required computational time and can be used in practice to numerically evaluate a large number of eigenfrequencies.

Compared with [16], this paper presents advances in several directions. First, we consider several other very important problems. In addition to Mathieu's system, discretization with spectral collocation in conjunction with numerical methods for the obtained algebraic MEP can be applied to Lamé's system as well as other MEPs that arise by separation of variables. To the best of our knowledge, this technique

Email addresses: bor.plestenjak@fmf.uni-lj.si (Bor Plestenjak), ghcalin@ictp.acad.ro (Călin I. Gheorghiu)
URL: www.win.tue.nl/∼hochsten/ (Michiel E. Hochstenbach)

has never been applied to these problems until now. In particular, in Example 5 we apply this method to a three-parameter eigenvalue problem (3EP) and compute eigenmodes of a challenging ellipsoidal wave equation.

Second, while a Jacobi–Davidson style solver [19, 20] and standard implicitly restarted Arnoldi [37] were used in [16] to solve the 2EPs, we speed up the computations in this paper even more by exploiting a new fast Sylvester–Arnoldi algorithm for 2EPs from [29]; this algorithm is briefly described in Section 6. Third, we compare with, and improve on several available results in the literature in the numerical examples in Section 7. Finally, we present a MATLAB toolbox for solving MEPs coming from various equations.

The rest of this paper is organized as follows. Section 2 provides several examples of the technique of separation of variables leading to MEPs. A generic form of such MEP is treated in Section 3. In Section 4 we give an overview of the spectral collocation method, which is used to discretize a MEP into an algebraic MEP. This eigenvalue problem is presented in Section 5. In Section 6 we give an overview of available numerical methods for algebraic MEPs with an emphasis on the recent Sylvester–Arnoldi method from [29]. An important part of the paper are the numerical examples in Section 7. In several examples we demonstrate that spectral collocation combined with the Sylvester–Arnoldi method can compute several hundreds of the smallest eigenmodes very efficiently and accurately; we hereby improve various previous results. In the appendix we describe the main functions in a freely available MATLAB toolbox MultiParEig that contains the implementations of all algorithms and numerical examples from this paper.

2. Motivating problems

Whenever the separation of variables is used to solve a boundary value problem related to a PDE, a system of ODEs is obtained in the first instance. Then, the boundary conditions of the problem at hand dictate boundary conditions for the unknowns of the systems of ODEs involved. Consequently, a MEP is now well defined.

In this section we give some examples of boundary value problems where separation of variables leads to MEPs. We do not attempt to describe all possible situations; for a good overview of all possible coordinate systems and related boundary value problems, see, e.g., [25, 30, 32, 46]. Additional examples together with numerical solutions can be found in Section 7.

2.1. Mathieu's system

This is probably the most well-known example of a 2EP. Separation of variables applied to the two-dimensional Helmholtz equation $\nabla^2 u + \omega^2 u = 0$ in elliptic coordinates

$$\begin{aligned} x &= h\cosh(\xi)\cos(\eta),\\ y &= h\sinh(\xi)\sin(\eta), \end{aligned}$$

where $0 \le \xi < \infty$ and $0 \le \eta < 2\pi$, leads to $u = G(\eta)F(\xi)$, where G and F satisfy the coupled system of Mathieu's angular and radial equations (for details, see, e.g., [41])

$$\begin{aligned} &G''(\eta) + (\lambda - 2\mu\cos(2\eta))G(\eta) = 0,\\ &F''(\xi) - (\lambda - 2\mu\cosh(2\xi))F(\xi) = 0. \end{aligned} \tag{1}$$

The parameter μ is related to the eigenfrequency ω by $\mu = \frac{1}{4}h^2\omega^2$, where $h = \sqrt{\alpha^2 - \beta^2}$ with $\alpha = h\cosh(\xi_0)$ (the major axis) and $\beta = h\sinh(\xi_0)$ (the minor axis of the membrane), and λ is a separation constant. The problem along with the appropriate boundary conditions is treated as a 2EP in [16] and solved numerically very accurately and efficiently with the Chebyshev collocation. As discussed in the introduction, we will extend the results in [16] considerably in several ways.

2.2. Lamé's system

When separation of variables is applied to the three-dimensional Helmholtz equation $\nabla^2 u + \omega^2 u = 0$ in sphero-conal coordinates

$$\begin{aligned} x &= r\cos(\varphi)\,(1-k'^2\cos^2(\theta))^{1/2},\\ y &= r\cos(\theta)\,(1-k^2\cos^2(\varphi))^{1/2},\\ z &= r\sin(\theta)\,\sin(\phi), \end{aligned}$$

where $r \geq 0$, $0 \leq \theta \leq 2\pi$, $0 \leq \phi \leq \pi$, $0 \leq k, k' \leq 1$, and $k^2 + k'^2 = 1$, it gives $u = R(r)L(\varphi)N(\theta)$, where R, L, and N satisfy the system of differential equations

$$r^2 R''(r) + 2rR'(r) + [\omega^2 r^2 - \rho\,(\rho+1)]R(r) = 0, \tag{2}$$

$$(1-k^2\cos^2(\varphi))L''(\varphi) + k^2\sin(\varphi)\cos(\varphi)L'(\varphi) + [k^2\rho\,(\rho+1)\sin^2(\varphi) + \delta]L(\varphi) = 0, \tag{3}$$

$$(1-k'^2\cos^2(\theta))N''(\theta) + k'^2\sin(\theta)\cos(\theta)N'(\theta) + [k'^2\rho\,(\rho+1)\sin^2(\theta) - \delta]N(\theta) = 0, \tag{4}$$

where $\rho\,(\rho+1)$ and δ are separation constants. System (3)–(4) is a trigonometric form of Lamé's pair of differential equations, which forms a 2EP together with boundary conditions. All three equations along with the boundary conditions form a 3EP; still, the main problem is to solve (3)–(4), as for each solution of this 2EP we can insert $\rho\,(\rho+1)$ in (2) and solve it. For details, see, e.g., [9], [24], or [46, Sect. 15]. When we start with the Laplace equation $\nabla^2 u = 0$, we get the same system as the above without the ω^2 term in (2).

2.3. Bessel wave equations

The solution of the three-dimensional Helmholtz equation $\nabla^2 u + \omega^2 u = 0$ in parabolic rotational coordinates

$$\begin{aligned} x &= \xi\,\eta\,\cos(\phi),\\ y &= \xi\,\eta\,\sin(\phi),\\ z &= \tfrac{1}{2}\,(\eta^2 - \xi^2), \end{aligned}$$

where $0 \leq \xi, \eta < \infty$ and $0 < \phi < 2\pi$, is $u = \Phi(\phi)M(\xi)N(\eta)$, where Φ, M, and N satisfy the system of differential equations

$$\Phi''(\phi) + k_3^2\,\Phi(\phi) = 0, \tag{5}$$

$$\xi^2 M''(\xi) + \xi M'(\xi) + (k_2\,\xi^2 + \omega^2\,\xi^4 - k_3^2)M(\xi) = 0, \tag{6}$$

$$\eta^2 N''(\eta) + \eta N'(\eta) - (k_2\,\eta^2 - \omega^2\,\eta^4 + k_3^2)N(\eta) = 0, \tag{7}$$

where k_2 and k_3 are separation parameters. A solution of (5) is $\Phi(\phi) = e^{ip\phi}$, where $p = \pm k_3$. Whenever a periodicity condition, i.e., $\Phi(0) = \Phi(2\pi)$, $\Phi'(0) = \Phi'(2\pi)$, is imposed to the solution of (5), the parameter p becomes an integer. When we fix $k_3 = p$, the remaining two equations (6)–(7) (known as the Bessel wave equations), subject to the appropriate boundary conditions, give a 2EP. For details see, e.g., [28] or [46, Sect. 14].

2.4. Lamé (ellipsoidal) wave equations

The solution of the three-dimensional Helmholtz equation $\nabla^2 u + \omega^2 u = 0$ in ellipsoidal coordinates [32, Sect. 29.18(ii)] is $u = u_1(\alpha)\,u_2(\beta)\,u_3(\gamma)$, where u_1, u_2, and u_3 satisfy the Lamé or ellipsoidal wave equations, which can be expressed in Jacobian form

$$\begin{aligned}
u_1''(\alpha) + [h - \nu\,(\nu+1)\,k^2\,\mathrm{sn}^2(\alpha,k) + k^2\,\omega^2\,\mathrm{sn}^4(\alpha,k)]\;u_1(\alpha) &= 0,\\
u_2''(\beta) + [h - \nu\,(\nu+1)\,k^2\,\mathrm{sn}^2(\beta,k) + k^2\,\omega^2\,\mathrm{sn}^4(\beta,k)]\;u_2(\beta) &= 0,\\
u_3''(\gamma) + [h - \nu\,(\nu+1)\,k^2\,\mathrm{sn}^2(\gamma,k) + k^2\,\omega^2\,\mathrm{sn}^4(\gamma,k)]\;u_3(\gamma) &= 0.
\end{aligned}$$

This system along with an appropriate set of boundary conditions gives a 3EP where each of the equations contains all three parameters. In [27] a numerical method is presented that can compute eigenvalues with a prescribed multi-index (the number of sign changes for each u_i). It is reported (see, e.g., [4, 45]) that the problem presents unusual computational difficulties and only recently some solutions were computed numerically in [45]. We show in Example 5 that it can be solved numerically quite efficiently by our multiparameter approach with spectral collocation.

2.5. System of spheroidal wave functions

The solution of the three-dimensional Helmholtz equation $\nabla^2 w + \omega^2 w = 0$ in prolate spheroidal coordinates [32, Sect. 30.13(iv)], [46, Sect. 12]) is $w = w_1(\xi)\,w_2(\eta)\,w_3(\phi)$, where w_1, w_2, and w_3 satisfy the system of differential equations

$$(1-\xi^2)\,w_1''(\xi) - 2\xi\,w_1'(\xi) + \left(\lambda + \gamma^2(1-\xi^2) - \frac{\mu^2}{1-\xi^2}\right) w_1(\xi) = 0, \tag{8}$$

$$(1-\eta^2)\,w_2''(\eta) - 2\xi\,w_2'(\eta) + \left(\lambda + \gamma^2(1-\eta^2) - \frac{\mu^2}{1-\eta^2}\right) w_2(\eta) = 0, \tag{9}$$

$$w_3''(\phi) + \mu^2\,w_3(\phi) = 0, \tag{10}$$

where $\gamma^2 = k^2 c^2 \geq 0$. This is a 3EP where two of the equations contain all three parameters and one equation contains just one. As before, if a periodicity condition $w_3(0) = w_3(2\pi)$, $w_3'(0) = w_3'(2\pi)$ is imposed to the solution of (10), then parameter μ becomes an integer.

The system (8)–(9) supplied with boundary conditions, for a fixed μ of order 1000 to 10000, is solved numerically as a 2EP in [3]. A similar system of spheroidal wave functions appears when separation of variables is applied to the three-dimensional Helmholtz equation in oblate spheroidal coordinates [32, Sect. 30.14(iv)], [46, Sect. 13].

3. Multiparameter boundary differential eigenvalue systems

An overview of the theory related to MEPs that are obtained by separation of variables is presented in [6]; see also [12, 36]. In the generic case separation of variables applied to a separable boundary value problem leads to a system of k differential equations of the form

$$\begin{aligned}
p_1(x_1)\,y_1''(x_1) + q_1(x_1)\,y_1'(x_1) + r_1(x_1)\,y_1(x_1) &= \lambda_1\,s_{11}\,y_1(x_1) + \cdots + \lambda_k\,s_{1k}(x_1)\,y_1(x_1)\\
&\;\;\vdots\\
p_k(x_k)\,y_k''(x_k) + q_k(x_k)\,y_k'(x_k) + r_k(x_k)\,y_k(x_k) &= \lambda_1\,s_{k1}\,y_k(x_k) + \cdots + \lambda_k\,s_{kk}(x_k)\,y_k(x_k)
\end{aligned} \tag{11}$$

together with the appropriate boundary conditions, where $k = 2$ or $k = 3$. We are interested in a k-tuple $(\lambda_1, \ldots, \lambda_k)$ and nontrivial functions $y_1, \ldots, y_k$ such that equations (11) and the boundary conditions are satisfied. In such case we say that $(\lambda_1, \ldots, \lambda_k)$ is an eigenvalue of (11). We remark that the numerical

methods from this paper are suitable for all problems of the form (11), regardless if they come from separation of variables or not.

If $x_i \in [a_i, b_i]$, then generic boundary conditions are

$$\alpha_i\, y_i(a_i) + \beta_i\, y_i'(a_i) = 0,$$
$$\gamma_i\, y_i(b_i) + \delta_i\, y_i'(b_i) = 0,$$

where $(\alpha_i, \beta_i) \neq (0,0)$ and $(\gamma_i, \delta_i) \neq (0,0)$ for $i = 1, \ldots, k$. In some cases boundary conditions can depend on eigenvalue parameters as well.

If the determinant $\delta(x_1, \ldots, x_k) := \det(s_{ij}(x_i))$ is definite for all $x_i \in [a_i, b_i]$, $i = 1, \ldots, n$, then it is well-known that the problem (11) is solvable, see, e.g., [6, 41]. In addition, the eigenvalues can be ordered by the multi-indices $(n_1, \ldots, n_k)$, which means that the corresponding eigenfunction $y_i(x_i)$ has exactly n_i zeros on (a_i, b_i) for $i = 1, \ldots, k$.

There exist some numerical methods for MEPs of the form (11). For problems that have additional definiteness properties, a continuation method is proposed in [2]; see also [23]. Once the problem (11) is discretized into an algebraic MEP, all methods from Section 6 can be applied.

Most of the numerical methods are limited to 2EPs, i.e., $k = 2$. A generalization of the shooting method is presented in [7] and a two-dimensional bisection is presented in [22]. A method using the Prüfer transformation that can compute an eigenvalue with a prescribed multi-index is presented in [1] for 2EPs and generalized to 3EPs, i.e., $k = 3$, in [26]. For some numerical methods for 3EPs see, e.g., [27] and the references therein.

4. Spectral methods

In this section we briefly introduce the spectral collocation method, which requires smaller matrices and returns more accurate results when compared with finite differences and finite elements methods. For more details, see, e.g., [10, 13, 15]. The spectral collocation method is based on approximating the solution $y(x)$ with a finite linear combination of a chosen set of orthogonal function as

$$y(x) \approx y_{N-1}(x) = \sum_{k=1}^{N} \alpha_k\, \varphi_k(x). \tag{12}$$

The coefficients $\alpha_1, \ldots, \alpha_N$ are chosen so that $y(x_i) = y_{N-1}(x_i)$ for $i = 1, \ldots, N$, where $x_1, \ldots, x_N$ are distinct collocation nodes. In this sense, $y_{N-1}(x)$ is an interpolating function for $y(x)$ on the set of collocation nodes. The large positive integer N is the order of approximation and is also called the cutoff parameter. To accommodate with physics, N can be viewed as the number of degrees of freedom (of modes) of a system.

Depending on the interval and other properties of the problem, various combinations of basis functions and collocation nodes exist. If the interval is finite, then a common choice is the set of Chebyshev polynomials as basis functions and collocation points are the Chebyshev nodes of the second kind. The method is called Chebyshev collocation (ChC) and the nodes on the interval $[-1, 1]$ are defined by

$$\xi_j = \cos\Big(\frac{(j-1)\pi}{N-1}\Big)$$

for $j = 1, \ldots, N$ (see, e.g., [42, Eq. (13)]).

As we have to discretize each of the equations of (11) independently, it is sufficient to consider one equation. Suppose that we have a differential equation

$$p(x)\, y''(x) + q(x)\, y'(x) + r(x)\, y(x) = \lambda\, s(x)\, y(x) + \mu\, t(x)\, y(x) \tag{13}$$

on the interval $[a,b]$. The ChC discretization of the above equation is

$$\left(\tfrac{4}{(b-a)^2}PD_N^2+\tfrac{2}{b-a}QD_N+R\right)f=\lambda Sf+\mu Tf, \tag{14}$$

where D_N and D_N^2 are first and second order differentiation matrices in the Chebyshev nodes of the second kind and $f=[y(x_1),\ldots,y(x_N)]^T$ is the vector of values in the collocation nodes

$$x_j=\tfrac{b-a}{2}\xi_j+\tfrac{a+b}{2}$$

for $j=1,\ldots,N$, which are translated from $[-1,1]$ to $[a,b]$. The matrices P, Q, R, S, and T are diagonal with diagonal elements $p(x_j)$, $q(x_j)$, $r(x_j)$, $s(x_j)$, and $t(x_j)$, respectively

We use the seminal paper [43] to obtain the entries of the differentiation matrices D_N and D_N^2; see also [11] for Maple code and [40] for MATLAB code. The matrices D_N and D_N^2 are dense, non-symmetric, and have much higher condition numbers as the corresponding symmetric tridiagonal finite difference matrices of the same size; see, e.g., [15, Fig. 3.13]. However, since discretization with the ChC requires much smaller matrices than with finite differences (see, e.g., [16, Ex. 5]), N is usually small enough so that the ill-conditioning is not an issue.

To impose the boundary conditions, we apply the simple and general strategy from [21]. Another option is used if boundary conditions depend on eigenvalue parameters. In such case we replace the first and the last equation of (14) with the equations from the boundary conditions. For instance, suppose that the boundary condition for (13) in point a is

$$(\alpha_1+\alpha_2\lambda+\alpha_3\mu)\,y(a)+(\beta_1+\beta_2\lambda+\beta_3\mu)\,y'(a)=0.$$

We write the above as

$$(\alpha+\alpha_2\lambda+\alpha_3\mu)\,[1\ 0\ \cdots\ 0]\,f+(\beta_1+\beta_2\lambda+\beta_3\mu)\,\tfrac{b-a}{2}\,D_N(1,:)\,f=0,$$

where $D_N(1,:)$ is the first row of D_N, and replace the first row of (14) with the above equation. We proceed similarly in point b.

In many cases the boundary conditions are *behavioral*, which means that they are satisfied implicitly by choosing basis functions that have the required property or behavior. For instance, suppose that the differential equation (13) has singularity at the endpoint a such that $p(a)=0$ and the boundary condition is that the solution should be bounded at a. As the Chebyshev polynomials (translated from $[-1,1]$ to $[a,b]$) are analytic at the endpoints, their sum satisfies the boundedness condition at $x=a$ and no additional explicit conditions are needed. Since collocation points in the ChC include the endpoints, the first equation of (14), which corresponds to the collocation point $x=a$, imposes the boundary condition at $x=a$ obtained from (13) by taking the limit $x\to a$. For more details, see [10, Section 6.3].

In case of the half line $[0,\infty)$ we use the Laguerre collocation (LC) (see, e.g., [15]). The basis functions are products of Laguerre polynomials and the weight function $e^{-\frac{1}{2}bx}$, where $b>0$ is the scaling parameter. The collocation nodes are $x_1=0<x_2/b<\cdots<x_N/b$, where $x_2,\ldots,x_N$ are the roots of the Laguerre polynomial L_{N-1} of degree $N-1$. When we use the LC, the boundary condition at infinity, which has to be $\lim_{x\to\infty}y(x)=0$, is automatically satisfied. The LC differentiation is exact for functions of the form $y(x)=e^{-\frac{1}{2}bx}p(x)$, where $p(x)$ is a polynomial of degree $\le N-1$. The scaling parameter b has to be carefully chosen according to how fast the solution decays to zero as $x\to\infty$.

5. Algebraic multiparameter eigenvalue problems

When we discretize the MEP (11) we obtain an algebraic MEP, which has the form

$$\begin{aligned} A_{10}x_1 &= \lambda_1 A_{11}x_1+\cdots+\lambda_k A_{1k}x_1\\ &\ \ \vdots\\ A_{k0}x_k &= \lambda_1 A_{k1}x_k+\cdots+\lambda_k A_{kk}x_k, \end{aligned} \tag{15}$$

where A_{ij} is an $n_i \times n_i$ complex matrix for $i = 1,\dots,k$ and $j = 0,\dots,k$. A k-tuple $(\lambda_1,\dots,\lambda_k)$ is an eigenvalue if it satisfies (15) for nonzero vectors $x_1 \in \mathbb{C}^{n_1},\dots,x_k \in \mathbb{C}^{n_k}$. The corresponding eigenvector is the tensor product $x_1 \otimes \cdots \otimes x_k$. Introducing the so-called $k \times k$ operator determinants

$$\Delta_0 = \begin{vmatrix} A_{11} & \cdots & A_{1k} \\ \vdots & & \vdots \\ A_{k1} & \cdots & A_{kk} \end{vmatrix}_{\otimes} \quad \text{and} \quad \Delta_i = \begin{vmatrix} A_{11} & \cdots & A_{1,i-1} & A_{10} & A_{1,i+1} & \cdots & A_{1k} \\ \vdots & & \vdots & \vdots & & & \vdots \\ A_{k1} & \cdots & A_{k,i-1} & A_{k0} & A_{k,i+1} & \cdots & A_{kk} \end{vmatrix}_{\otimes}$$

for $i = 1,\dots,k$, where the Kronecker product $\otimes$ is used instead of multiplication, we obtain matrices $\Delta_0,\dots,\Delta_k$ of size $n_1 \cdots n_k \times n_1 \cdots n_k$. If Δ_0 is nonsingular, then the matrices $\Delta_0^{-1}\Delta_1,\dots,\Delta_0^{-1}\Delta_k$ commute and (15) is equivalent (for details, see, e.g., [5]) to a system of generalized eigenvalue problems

$$\begin{array}{rcl} \Delta_1 z & = & \lambda_1 \Delta_0 z, \\ & \vdots & \\ \Delta_k z & = & \lambda_k \Delta_0 z \end{array} \tag{16}$$

for decomposable tensors $z = x_1 \otimes \cdots \otimes x_k$. This relation enables one to use standard numerical methods for the computation of eigenvalues if the Δ-matrices are not too large. However, when we use spectral methods to discretize (11), then usually even for $k = 2$ the Δ-matrices are so large that it is not efficient or even not feasible to compute all the eigenvalues. The available numerical methods are presented in the next section.

Let us mention that if we discretize a self-adjoint MEP (11) obtained via the separation of variables using the spectral collocation method from Section 4, then the algebraic MEP is solvable, although it is not self-adjoint (since matrices D_N and D_N^2 are not symmetric). Namely, the matrices A_{ij} for $i, j = 1,\dots,k$ are all diagonal and if $\delta(x_1,\dots,x_k) := \det(s_{ij}(x_i))$ is definite for all $x_i \in [a_i, b_i]$, $i = 1,\dots,n$, then the corresponding operator determinant Δ_0 is nonsingular.

Example 1. For future reference, we give (15) and the corresponding operator determinants for the case $k = 2$. An algebraic 2EP has the form

$$\begin{aligned} A_1 x_1 &= \lambda B_1 x_1 + \mu C_1 x_1 \\ A_2 x_2 &= \lambda B_2 x_2 + \mu C_2 x_2. \end{aligned} \tag{17}$$

The eigenvalue is a pair (λ, μ) which satisfies (17) for nonzero vectors x_1 and x_2. The corresponding 2×2 operator determinants of size $n_1 n_2 \times n_1 n_2$ are

$$\begin{array}{rcl} \Delta_0 & = & B_1 \otimes C_2 - C_1 \otimes B_2, \\ \Delta_1 & = & A_1 \otimes C_2 - C_1 \otimes A_2, \\ \Delta_2 & = & B_1 \otimes A_2 - A_1 \otimes B_2. \end{array} \tag{18}$$

If Δ_0 is nonsingular, then $\Delta_0^{-1}\Delta_1$ and $\Delta_0^{-1}\Delta_2$ commute and (17) is equivalent to a coupled pair of generalized eigenvalue problems

$$\begin{aligned} \Delta_1 z &= \lambda \Delta_0 z, \\ \Delta_2 z &= \mu \Delta_0 z \end{aligned} \tag{19}$$

for decomposable tensors $z = x_1 \otimes x_2$. This will be used in all our numerical examples.

6. Numerical methods

If the size $n_1 \cdots n_k$ of the Δ-matrices in (16) is small enough, say $n_1 \cdots n_k \leq 1000$ on a typical laptop, we can efficiently compute all eigenvalues of a MEP (15) from the related system of generalized eigenvalue problems (16). This numerical algorithm, which is based on the QZ algorithm, is given in Algorithm 1. It was presented in [19] for $k = 2$, and can be generalized in a straightforward way to three or more parameters. The MATLAB toolbox MultiParEig that we describe in the appendix contains implementations of Algorithm 1 and its generalization for $k = 3$.

Algorithm 1 An algorithm for the nonsingular two-parameter eigenvalue problem (17).

1. Compute a generalized Schur decomposition $Q^H \Delta_0 Z = R$ and $Q^H \Delta_1 Z = S$, such that Q and Z are unitary, R and S are upper triangular, and multiple values of $\lambda_i := s_{ii}/r_{ii}$ are clustered along the diagonal of $R^{-1}S$. As a result, R and S are partitioned as

$$R = \begin{bmatrix} R_{11} & R_{12} & \cdots & R_{1p} \\ 0 & R_{22} & \cdots & R_{2p} \\ \vdots & \vdots & \ddots & \vdots \\ 0 & 0 & \cdots & R_{pp} \end{bmatrix}, \quad S = \begin{bmatrix} S_{11} & S_{12} & \cdots & S_{1p} \\ 0 & S_{22} & \cdots & S_{2p} \\ \vdots & \vdots & \ddots & \vdots \\ 0 & 0 & \cdots & S_{pp} \end{bmatrix},$$

   where the size of R_{ii} and S_{ii} is m_i and $m_1 + \cdots + m_p = n_1 n_2$.
2. Compute diagonal blocks $T_{11}, \ldots, T_{pp}$ of $T = Q^H \Delta_2 Z$.
3. Compute the eigenvalues $\mu_{i1}, \ldots, \mu_{im_i}$ of $T_{ii} w = \mu R_{ii} w$ for $i = 1, \ldots, p$.
4. The eigenvalues of (17) are $(\lambda_1, \mu_{11}), \ldots, (\lambda_1, \mu_{1m_1}); \ldots; (\lambda_p, \mu_{p1}), \ldots, (\lambda_p, \mu_{pm_p})$.
5. For each eigenvalue (λ, μ) compute the eigenvector $x_1 \otimes x_2$ by inverse iteration on $A_i - \lambda B_i - \mu C_i$ for $i = 1, 2$.

If $n_1 \cdots n_k$ is too large then it is not efficient or even not feasible to compute all the eigenvalues. Instead, we can compute a subset of eigenvalues by an iterative method. For $k = 2$, if we are looking for eigenvalues (λ, μ) close to a given target (σ, τ), then a method of choice is the harmonic version [20] of the Jacobi–Davidson method [19], which can also be easily generalized to three or more parameters. For an overview of other numerical methods, see, e.g., [19] and references therein.

In the remainder we will focus on numerical methods for 2EPs. Recently, a set of algorithms was presented in [29] that are very suitable for 2EPs related to separable boundary value problems. In many applications, for instance when we consider the Helmholtz equation $\nabla^2 u + \omega^2 u = 0$, only one of the eigenvalue parameters λ and μ is related to ω and thus relevant. Without loss of generality we can assume that this parameter is μ. In a typical situation we are interested in a number m of the lowest eigenfrequencies ω and the corresponding eigenmodes. Usually, the problem can be reformulated in such way that we have to find the m eigenvalues (λ, μ) with the smallest $|\mu|$.

While a problem (11) usually has infinitely many eigenvalues, each discretization (17) has only finitely many eigenvalues. We may expect that some of them are good approximations to the eigenvalues of (11) while the remaining ones contain no useful information. For one-parameter problems, a heuristic suggested in [10, Rule-of-Thumb 8, p. 132] states:

> *In solving a linear eigenvalue problem by a spectral method using $N + 1$ terms in the truncated spectral series, the lowest $\frac{1}{2}N$ eigenvalues are usually accurate to within a few percent while the larger $\frac{1}{2}N$ numerical eigenvalues differ from those of differential equation by such large amounts as to be useless.*

Much time and energy has been spent along the last decades in the invention of slight modifications to standard spectral methods in order to solve the "spurious eigenvalue" difficulty (see, e.q., [18] and [10, Sections 7.5 and 7.6]). On one hand there are *physically spurious eigenvalues* that are numerically-computed ones which are in error because of misapplication of boundary conditions or some other misrepresentation of the physics. The original continuous MEPs that we consider are self-adjoint, physically well established, and consequently the appearance of such spurious eigenvalues is highly unlikely. On the other hand we can always expect some *numerically spurious eigenvalues* that are poor approximation to exact eigenvalues because the mode is oscillating too rapidly to be resolved by N degrees of freedom. Such numerically spurious eigenvalue can be computed accurately by using sufficiently large N. This explains the fairly high accuracy in computing the "smallest" eigenvalue for a self-adjoint problem with target oriented algorithms.

As a reliable test it is suggested in [10] to repeat the calculations with different N and compare the results. It is also noted that the number of good eigenvalues may be smaller if the modes have boundary layers, critical levels, or other areas of very rapid change, or when the interval is unbounded. We will not discuss the convergence here, but, as we increase the sizes of the matrices in (17), more and more eigenvalues of (17) should converge to exact eigenvalues of (11) and the eigenvalues with the smallest value of $|\mu|$ typically converge among first.

The sizes n_1 and n_2 depend on the number m of the wanted lowest eigenfrequencies and on the required accuracy. Usually $m \ll n_1 n_2$ and if $n_1 n_2$ is small, we can compute all values μ from the generalized eigenvalue problem $\Delta_2 z = \mu \Delta_0 z$. If $n_1 n_2$ is too large for Algorithm 1, then we can apply the implicitly restarted Arnoldi method [37], Krylov–Schur method [38], or any other iterative method based on Krylov subspaces, to the matrix $\Gamma_2^{-1} := \Delta_2^{-1}\Delta_0$. To do this, we must be able to efficiently multiply by Γ_2^{-1}, i.e., to solve a system

$$\Delta_2 w = \Delta_0 z \tag{20}$$

for a given vector z. In principle, the complexity of the above step is $\mathcal{O}(n_1^3 n_2^3)$ as the matrices Δ_0, Δ_1, and Δ_2 are of size $n_1 n_2 \times n_1 n_2$. But, by formulating (20) as a Sylvester equation, we can solve it in $\mathcal{O}(n_1^3 + n_2^3)$. The key to the big reduction is the well-known equality

$$(A \otimes B)\,\mathrm{vec}(X) = \mathrm{vec}(BXA^T),$$

which enables us to write (20), i.e., $(B_1 \otimes A_2 - A_1 \otimes B_2)\, w = (B_1 \otimes C_2 - C_1 \otimes B_2)\, z$, as

$$A_2 W B_1^T - B_2 W A_1^T = C_2 Z B_1^T - B_2 Z C_1^T =: M,$$

where $z = \mathrm{vec}(Z)$ and $w = \mathrm{vec}(W)$. We get the Sylvester equation

$$A_2^{-1} B_2 W - W B_1^T A_1^{-T} = -A_2^{-1} M A_1^{-T},$$

which can be solved in $\mathcal{O}(n_1^3 + n_2^3)$ by the Bartels–Stewart algorithm [8]. The overall algorithm from [29], which is included in MATLAB toolbox MultiParEig, is given in Algorithm 2.

Here we give some additional explanation about Algorithm 2, for more details see [29]. The algorithm requires that A_1 and A_2 are both nonsingular. If this is not the case, then it follows from [29, Lemma 3.1] that there exists θ such that $A_1 - \theta B_1$ and $A_2 - \theta B_2$ are both nonsingular. When we find such θ, which is not difficult as there are only finitely many inappropriate values, we apply the shift $\lambda = \widetilde{\lambda} + \theta$ and use Algorithm 2 on the shifted problem

$$\begin{aligned} (A_1 - \theta B_1)\, x_1 &= \widetilde{\lambda}\, B_1 x_1 + \mu\, C_1 x_1 \\ (A_2 - \theta B_2)\, x_2 &= \widetilde{\lambda}\, B_2 x_2 + \mu\, C_2 x_2. \end{aligned} \tag{21}$$

Algorithm 2 A Sylvester–Arnoldi method for the nonsingular two-parameter eigenvalue problem (17) with nonsingular Δ_2. The algorithm returns eigenvalues of $\Delta_2 z = \mu \Delta_0 z$ with the smallest absolute value and the corresponding invariant subspace.

1. Compute Schur decompositions $A_2^{-1}B_2 = U_1 R_1 U_1^H$ and $B_1^T A_1^{-T} = U_2 R_2 U_2^H$.
2. Apply implicitly restarted Arnoldi or Krylov–Schur method on $\Gamma_2^{-1} := \Delta_2^{-1}\Delta_0$, where in each step the product $w = \Gamma_2^{-1} z$ is computed as:
   (a) set matrix Z such that $z = \mathrm{vec}(Z)$
   (b) solve Sylvester equation $R_1 W - W R_2 = -U_1^H A_2^{-1} Z A_1^{-T} U_2$
   (c) $w = \mathrm{vec}(W)$

Once we have an eigenpair (μ, z) of $\Delta_2 z = \mu \Delta_0 z$, it is easy to compute the eigenvalue (λ, μ) and the vectors x_1 and x_2 of (17). The eigenvector $z = x_1 \otimes x_2$ is decomposable and if $z = \mathrm{vec}(Z)$, then Z has rank one and $Z = x_2 x_1^T$. Thus, we can extract x_1 and x_2 from the singular value decomposition of Z. From x_1 and x_2 the eigenvalue parameter λ can be computed from the tensor Rayleigh quotient [34] efficiently as

$$\lambda = \frac{z^H \Delta_1 z}{z^H \Delta_0 z} = \frac{(x_1^H A_1 x_1)(x_2^H C_2 x_2) - (x_1^H C_1 x_1)(x_2^H A_2 x_2)}{(x_1^H B_1 x_1)(x_2^H C_2 x_2) - (x_1^H C_1 x_1)(x_2^H B_2 x_2)}.$$

In the case of three or more parameters, we are not aware of a method that reduces the complexity of solving the linear system with the Δ-matrices in a similar way as in Algorithm 2; this is left for future research. We can apply any iterative method based on Krylov subspaces on the Δ-matrices, but since we use full vectors of size $n_1 \cdots n_k$, we cannot use as many collocation points as for 2EPs.

7. Numerical examples

In this section we give some numerical examples that show the strengths of the proposed approach and explain some further details. From the literature we take several boundary value problems that lead to some 2EPs and one 3EP, and solve them numerically with the methods proposed in the paper using MATLAB toolbox MultiParEig [35]. In many cases our numerical results are more accurate than the previously reported in the literature and we also give more eigenmodes. Fast computational times show that it is possible to numerically solve many separable boundary value problems efficiently as MEPs.

The following numerical examples were obtained on 64-bit Windows version of Matlab R2012b running on Intel(R) Core(TM) i5-4670 3.40Ghz processor and 16 GB of RAM.

Example 1. In the first example, which is based on [31], we consider Lamé's system (see Subsection 2.2), related to the problem of computing the strength of a charge singularity of a flat plate for corner angle $0 < \chi < 2\pi$:

$$[1 - k^2\cos^2(\varphi)]L''(\varphi) + k^2 \sin(\varphi)\cos(\varphi)L'(\varphi) + [k^2\rho(\rho+1)\sin^2(\varphi) + \delta]L(\varphi) = 0, \tag{22}$$

$$[1 - k'^2\cos^2(\theta)]N''(\theta) + k'^2 \sin(\theta)\cos(\theta)N'(\theta) + [k'^2\rho(\rho+1)\sin^2(\theta) - \delta]N(\theta) = 0, \tag{23}$$

where $r \geq 0$, $0 \leq \theta \leq 2\pi$, $0 \leq \phi \leq \pi$, $0 \leq k, k' \leq 1$, and $k^2 + k'^2 = 1$. Since the problem is located in the half-space $z \geq 0$, the range of θ can be reduced to $[0, \pi]$. For the solution $N(\theta)$ it either holds $N(\pi - \theta) = N(\theta)$ so that $N'(\pi/2) = 0$, or $N(\pi - \theta) = -N(\theta)$ and hence $N(\pi/2) = 0$. Therefore, it suffices to consider $\theta \in [0, \frac{\pi}{2}]$. The relevant boundary conditions for our case are $L(0) = L'(\pi) = 0$ and $N'(0) = N'(\pi/2) = 0$ if $0 < \chi < \pi$ or $N(0) = N'(\pi/2) = 0$ if $\pi < \chi < 2\pi$. The goal is to compute the smallest $\rho > 0$ for $k = \sin(|\pi - \chi|/2)$. This problem is solved numerically as a 2EP in [29] using finite

differences, where quite large matrices (of size 40000×40000) are needed for accurate results. Using the ChC discretization more accurate results can be obtained with much smaller matrices.

We set $\lambda = \delta$, $\mu = \rho\,(\rho+1)$ and discretize (22) and (23) using the ChC. In the discretized problem (17), A_1 and A_2 are full, C_1 and C_2 are diagonal, and $-B_1$ and B_2 are identity matrices. Due to the boundary conditions, matrices A_2, C_1, and C_2 are singular. We fix this by shifting λ so that we can apply the implicitly restarted Arnoldi version of Algorithm 2. We take the rather arbitrary shift $\lambda = \widetilde{\lambda} - 10$ and then numerically solve the shifted problem (21) for $\theta = -10$. Numerical experiments show that the use of 60 collocation points for each equation is sufficient to compute the ten smallest values ρ to at least 8 accurate digits. All values, when rounded, agree to the values in [31, Tabs. 1 and 2], which are given with 4 or 5 digits. The same problem is solved in [7] with the shooting method and in [22] with the two-dimensional bisection method, they both report the corresponding values μ. In Table 1 we give values for some corner angles χ for comparison. The remaining values can be computed using the function demo_lame in toolbox MultiParEig. Let us note that the computation of all values ρ and μ (for 31 different values of χ) takes just 0.6 seconds.

Table 1: Solutions of charge-singularity problem (22)–(23), computed by the ChC on 60 points and Algorithm 2 (second and fourth column), compared with the values obtained in [31] (third column), [7] (fifth column), and [22] (sixth column).

	$\rho = (-1+\sqrt{1+4\mu})/2$		μ		
χ/π	ChC and Alg. 2	Morrison and Lewis [31]	ChC and Alg. 2	Bailey [7]	Ji [22]
0.04021	0.12003200	0.12003	0.13443968	0.1344183	0.1344238
0.11610	0.16041747	0.16042	0.18615124	–	–
0.28858	0.22487941	0.22488	0.27545016	0.2754502	0.2753945
0.950	0.47560917	0.47561	0.70181325	–	0.7025342
1.125	0.64219762	0.6422	0.88771014	0.8877101	0.8876282
1.500	0.81465525	0.8146	1.47831844	–	–
1.875	0.98991459	0.98991	1.96984549	–	1.971277
1.950	0.99844224	0.99844	1.99532914	–	1.995327

To explore the convergence, we compute the first 700 eigenvalue parameters $\mu = \rho(\rho+1)$ of Lamé's system (22)–(23) by the ChC discretization using $N = 30, 40, \ldots, 110$ points and Algorithm 2. For the "exact" values we take the solutions obtained for $N = 150$. The errors for two corner angles ($\chi = 0.04021\pi$ for the left figure and $\chi = \frac{1}{2}\pi$ for the right figure) are visualized in Figure 1 and clearly show the convergence of the ChC. Each rectangle corresponds to a group of 20 consecutive values μ on the y-axis and one choice of N from the x-axis. The color of the rectangle depicts the maximum relative error of the eigenvalues in the group. In both cases, as we enlarge N, more and more eigenvalues are computed accurately and their number seems to grow at least linearly with N. One can see that more collocation points are required to compute low eigenfrequencies accurately for a sharper corner angle in the left figure. Algorithm 2 requires 91 seconds to compute the first 700 eigenmodes for $N = 110$.

Example 2. We consider a 2EP from [28], which appears when the separation of variables is applied to the Helmholtz equation in parabolic rotational coordinates for a closed region bounded by two paraboloids $\xi = \xi_0$ and $\eta = \eta_0$ (see Subsection 2.3), which has the volume

$$V = \tfrac{\pi}{4}\ \xi_0^2\ \eta_0^2\ (\xi_0^2 + \eta_0^2).$$

The corresponding 2EP consists of the Bessel wave equations

$$\xi^2 M''(\xi) + \xi M'(\xi) + (k_2\xi^2 + \omega^2\xi^4 - p^2)M(\xi) = 0, \tag{24}$$

$$\eta^2 N''(\eta) + \eta N'(\eta) - (k_2\eta^2 - \omega^2\eta^4 + p^2)N(\eta) = 0. \tag{25}$$

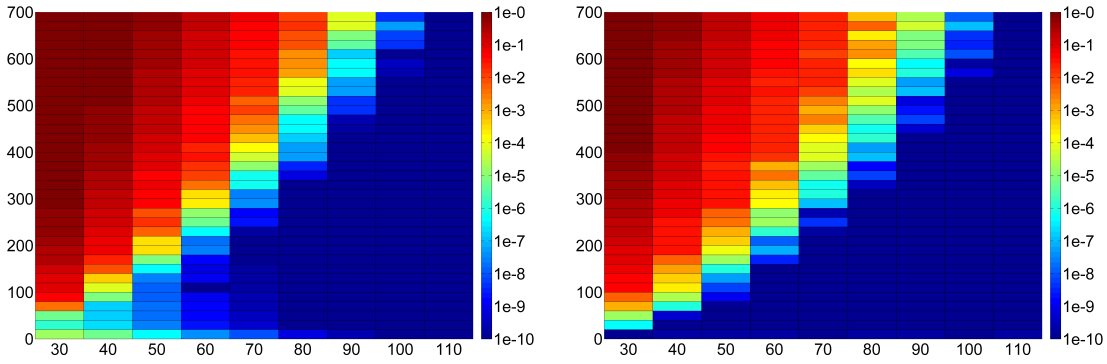

Figure 1: Convergence of the ChC applied to (3)–(4) for $\chi = 0.04021\pi$ (left) and $\chi = \pi/2$ (right), as a function of the number of collocation points (horizontal) and the number of the eigenmode (vertical axis).

and appropriate boundary conditions, where we can consider only nonnegative integer values of p. In the case $p = 0$, which is treated separately, we divide (24) and (25) by ξ and η, respectively, to obtain

$$\xi M''(\xi) + M'(\xi) + (k_2\xi + \omega^2\xi^3)M(\xi) = 0, \tag{26}$$

$$\eta N''(\eta) + N'(\eta) - (k_2\eta - \omega^2\eta^3)N(\eta) = 0. \tag{27}$$

The solutions of the Helmholtz equation should be bounded in the physical domain. The equations (24)–(25) for $p \geq 1$ and (26)–(27) for $p = 0$ have regular singularities at $\xi = 0$ and $\eta = 0$. The boundedness conditions at these singular points are behavioral and are automatically satisfied in the ChC, where we take the set of Chebyshev polynomials as basis functions in the expansion (12). Actually, this expansion provides an analytic approximation. It follows from (24)–(25) and (26)–(27) that bounded solutions satisfy $M(0) = N(0) = 0$ for $p \geq 1$ and $M'(0) = N'(0) = 0$ for $p = 0$, respectively. Equations with the above boundary conditions appear in the ChC as the equations at the collocation points $\xi = 0$ and $\eta = 0$. Three possible combinations of outer boundary conditions are considered: Dirichlet ($M(\xi_0) = N(\eta_0) = 0$), Neumann ($M'(\xi_0) = N'(\eta_0) = 0$), and mixed ($M(\xi_0) = 0 = N'(\eta_0) = 0$).

Similar to the previous example, we set $\lambda = k_2$, $\mu = \omega^2$ and discretize the system using the ChC on 60 points. For each $p = 0, \ldots, 8$ we compute 8 eigenvalues with the smallest ω and then gather the results. In Table 2 we give the first ten eigenvalues with the smallest ω for the Dirichlet case, while in Figure 2 we plot the first nine eigenmodes in the xy-plane for the Dirichlet case. More eigenvalues can be computed using function demo_besselwave1 in MultiParEig, which also gives the eigenvalues for the Neumann and the mixed case.

Based on numerical experiments with higher number of collocation nodes, which show a similar convergence as in Figure 1, 60 points should be enough for the results in Table 2 to have at least 8 accurate digits. Some of the solutions can be computed analytically. If γ is a positive zero of the Bessel function of the first kind $J_{p/2}(x)$, then $(\lambda, \omega) = (0, 2\gamma)$ is an eigenvalue of (24)–(25). The corresponding eigenfunctions that satisfy the boundary conditions are $M(\xi) = J_{p/2}(\gamma\xi^2)$ and $N(\eta) = J_{p/2}(\gamma\eta^2)$. These values agree perfectly with the eigenfrequencies in Table 2 where $\lambda = 0$. We also verified the numerical results by solving numerically each of the equations (24) and (25) as a one-parameter eigenvalue problem with a fixed value of either k_2 or ω by a shooting method in Mathematica. Based on these results we believe that the values obtained by discretizing the problem with the ChC as a 2EP are more accurate than the results obtained by the Frobenius power series expansion method in [28].

In Figure 3 we give the energy E of an electron in a quantum dot, computed as

$$E = \frac{\hbar^2\omega^2}{2m^H},$$

Table 2: Extended Table 1 from [28] with solutions for Dirichlet outer boundary conditions and $\xi_0^2 = \eta_0^2 = 1$, recomputed as solutions of the 2EP obtained by discretizing Bessel wave equations (24)–(25) by the ChC using 60 points (second column), compared with the values obtained in [28] by the Frobenius method (third column).

	ChC and Algorithm 2		Lew Yan Voon and Willatzen [28]	
p	λ	ω	λ	ω
0	0.00000000	4.80965112	0	4.809
1	0.00000000	6.28318531	0	6.286
2	0.00000000	7.66341194	0	7.665
0	13.46679582	7.87276640	13.468	7.875
3	0.00000000	8.98681892	0	8.974
1	21.73191565	9.35647141	–	–
4	0.00000000	10.27124460	–	–
2	29.69012955	10.77286063	–	–
0	39.97421371	10.89209896	–	–
0	0.00000000	11.04015622	–	–

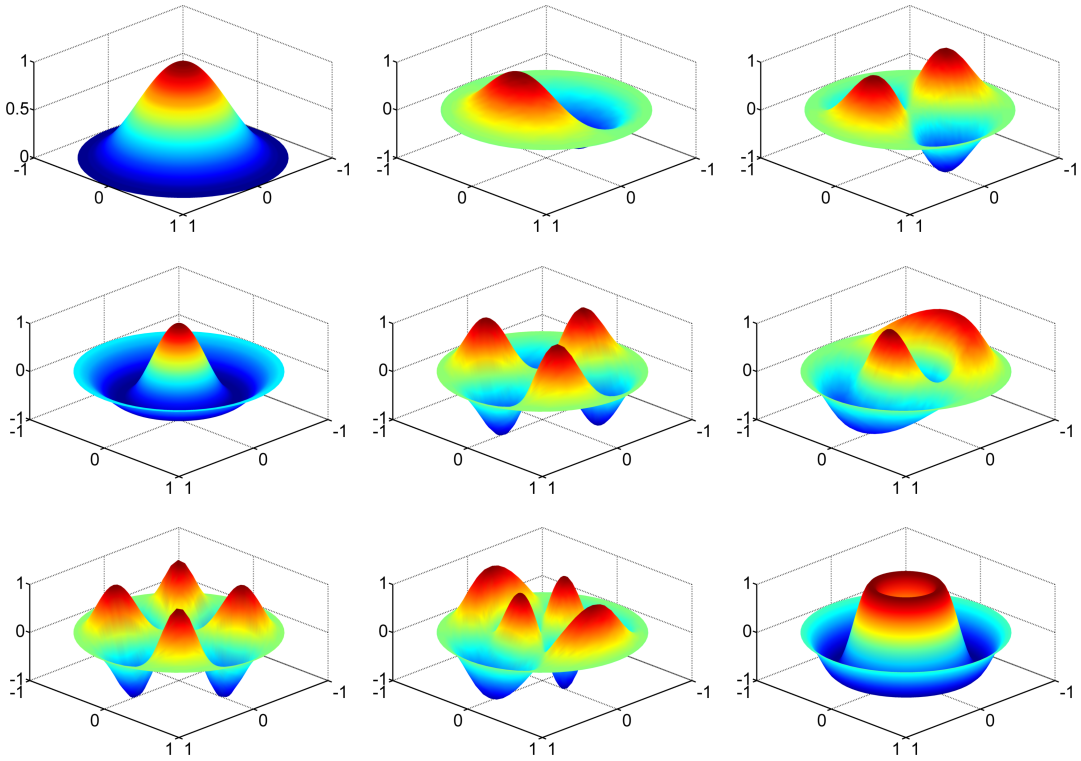

Figure 2: 3-D plots of the first nine eigenmodes from Table 2 for the symmetric region with $\xi_0^2 = \eta_0^2 = 1$ in the plane $z = 0$. The corresponding values of parameters (p, ω) are (from left to right, starting at the top row) $(0, 4.809)$, $(1, 6.283)$, $(2, 7.664)$, $(0, 7.873)$, $(3, 8.987)$, $(1, 9.356)$, $(4, 10.271)$, $(2, 10.773)$, and $(0, 10.892)$.

where $m^H = 0.067 m_0$ is the effective mass of an electron in GaAs and $\hbar$ is Planck's constant, as a function of ξ_0^2 for a serious of quantum dots having the same volume (see [28] for details). The graph is much smoother than [28, Fig. 5], which represents the same results. The figure is based on numerical computation of energy for 100 equidistant values of ξ_0^2, where we use the ChC discretization on 60 points to compute the energy for each ξ_0^2. The computation of the figure takes 2.3 seconds. The minimal energy 245.1379 meV is obtained at $\xi_0^2 = 19.0534$ Å and $\xi_0^2 = 180.4595$ Å.

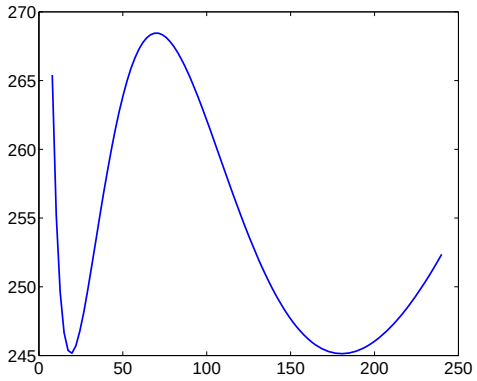

Figure 3: Ground state energy (in meV) related to ξ_0^2 (in Å) for various quantum dots of the same volume $5.39 \cdot 10^5$ Å^3 as in the symmetric case $\xi_0^2 = \eta_0^2 = 70$ Å.

Example 3. When separation of variables is applied to the three-dimensional Helmholtz equation $\nabla^2 u + \omega^2 u = 0$ in parabolic cylinder coordinates

$$\begin{aligned} x &= \tfrac{1}{2}(\mu^2 - \nu^2), \\ y &= \mu\,\nu, \\ z &= z, \end{aligned}$$

where $0 \le \mu < \infty$ and $-\infty < \nu, z < \infty$, then the system of ordinary differential equations

$$M''(\mu) - (\alpha + \beta\,\mu^2) M(\mu) = 0, \tag{28}$$

$$N''(\nu) + (\alpha - \beta\,\nu^2) N(\nu) = 0, \tag{29}$$

$$Z''(z) + (\omega^2 + \beta) Z(z) = 0 \tag{30}$$

is obtained, where α and β are separation parameters. Pair (28)–(29) with the corresponding boundary conditions is a 2EP in the form of the Weber equations. For each solution of (28)–(29) we can insert β in (30) and solve it to obtain the solution $u = M(\mu) N(\eta) Z(z)$. For details see, e.g., [32, Sect. 12], [44], or [46, Sect. 10].

In this numerical example, which is based on [44], we compute eigenmodes and eigenfrequencies of an acoustic enclosure defined by two confocal parabolic cylinders $|\nu| = \nu_0$ and $\mu = \mu_0$, and two plane surfaces $z = z_1$ and $z = z_2$, subject to rigid-wall boundary conditions. When we take $z_2 = -z_1 = L/2$, then solutions of (30) either have the form

$$Z(z) = \cos((\omega^2 - \beta)^{1/2} z),$$

where $\omega^2 = (2p)^2 (\pi/L)^2 - \beta$ for $p = 0, 1, 2, \ldots$; or

$$Z(z) = \sin((\omega^2 - \beta)^{1/2} z),$$

where $\omega^2 = -\beta$ or $\omega^2 = (2p+1)^2 (\pi/L)^2 - \beta$ for $p = 0, 1, 2, \ldots$. All eigenvalues (α, β) of the 2EP (28)–(29) have $\beta < 0$, therefore, when we want to compute the first eigenmodes, we have to find the solutions with the largest values of β. The solutions of the Helmholtz equation should be either odd or even in relation to the Cartesian axes z, hence the boundary conditions at 0 are either $M(0) = N(0) = 0$ or $M'(0) = N'(0) = 0$. It suffices to consider $0 < \nu < \nu_0$. The physical fluid rigid-wall interaction conditions imply the following boundary conditions $M'(\mu_0) = N'(\nu_0) = 0$ at μ_0 and ν_0.

In Table 3 we give the six eigenvalues (α,β) with the largest values of β for the odd and for the even case, more eigenvalues can be computed by function demo_weber in MultiParEig. The values in [44], obtained by the Frobenius method, are $(0,-4.4817)$ for the odd and $(\pm 6.037,-13.47)$ for the even case. Again, the values obtained by the ChC discretization are more accurate, which was verified numerically in Mathematica similarly as in the previous example. Some of the solutions are degenerate, i.e., they appear in pairs (α,β) and $(-\alpha,\beta)$.

Table 3: Eigenvalues (α,β) of the 2EP (28)–(29) for $\mu_0=\nu_0=1$ with the largest value of β, obtained by discretizing the equations by the ChC with 60 points, followed by Algorithm 2.

Odd case		Even case	
α	β	α	β
0.00000000	−4.48175894	0.00000000	0.00000000
±13.75247413	−26.66205565	±5.91160168	−13.30733575
±41.16966125	−65.31311007	±25.68754363	−43.94136005
0.00000000	−73.41246828	0.00000000	−48.74855787
±83.18622547	−120.03121747	±60.34249309	−90.68077098
±21.79442178	−136.62550800	±11.60150973	−102.65960842

In Figure 4 we plot the first nine nontrivial eigenmodes. As the solutions of degenerate pairs are symmetric, we give only one eigenmode for each such pair.

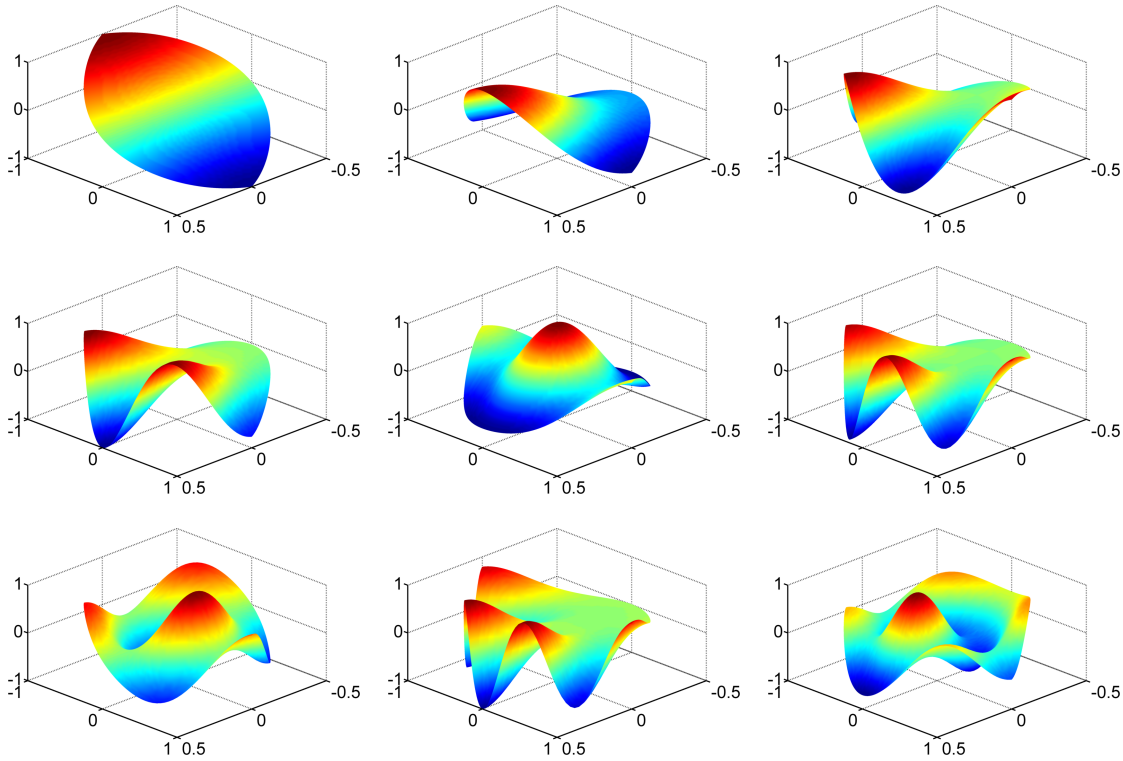

Figure 4: 3-D plots of the first nine nontrivial eigenmodes for the acoustic enclosure problem defined by two confocal parabolic cylinders $\mu_0=\nu_0=1$. The corresponding values of parameters (α,β) are (from left to right, starting at the top row) $(0,4.4817)$, $(5.9116,-13.3073)$, $(13.7525,-26.6621)$, $(25.6875,-43.9414)$, $(0,-48.7486)$, $(41.1697,-65.3131)$, $(0,-73.4125)$, $(60.3425,-90.6808)$, and $(11.6015,-102.6596)$.

Example 4. In [33], the energy eigenfunctions of hydrogen molecular ion H_2^+ in two dimensions in terms of confocal elliptic coordinates are considered. Separation of variables, applied to the Schrödinger equation for H_2^+ in two dimensions, leads to the system of differential equations

$$\begin{aligned}(u^2-1)\,F''(u)+u\,F'(u)+2Ru\,F(u)+\tfrac{1}{2}R^2E\,(u^2-1)\,F(u)-SF(u)=0,\\ (1-v^2)\,G''(v)-v\,G'(v)+\tfrac{1}{2}R^2E\,(1-v^2)\,G(v)+SG(v)=0,\end{aligned}$$

where $R>0$ is a given internuclear separation, E is the electronic energy, S is the separation constant, $1<u<\infty$, and $-1<v<1$. By taking $F(u)=(u^2-1)^{k/2}f(u)$ and $G(v)=(1-v^2)^{k/2}g(v)$, where $k=0$ or $k=1$, we separate out the singularities at $u^2=1$ and $v^2=1$, and obtain a new system of differential equations

$$(u^2-1)\,f''(u)+(2k+1)\,u\,f'(u)+\left(k+2Ru+\tfrac{1}{2}R^2E\,(u^2-1)-S\right)f(u)=0, \tag{31}$$

$$(v^2-1)\,g''(v)+(2k+1)\,v\,g'(v)+\left(k+\tfrac{1}{2}R^2E\,(v^2-1)-S\right)g(v)=0. \tag{32}$$

If for a pair (S,E) there exist bounded nontrivial functions $f(u)$ and $g(v)$ that satisfy (31) and (32), then (S,E) is an eigenvalue of the corresponding 2EP. We are interested in eigenvalues that have the smallest values of E and the matching eigenfunctions. We discretize the angular equation (32) by the ChC and apply the LC (shifted from $[0,\infty)$ to $[1,\infty)$) to the radial equation (31). The boundedness of the solution $f(u)$ to the radial equation (31) provides the boundary condition

$$\lim_{u\to\infty} f(u)=0, \tag{33}$$

which is automatically satisfied in the LC discretization, where we take the set of Laguerre polynomials multiplied by the weight function $w(x)=e^{-\frac{1}{2}bx}$ as basis functions in the expansion (12), and the boundary condition

$$(2k+1)\,f'(1)=-(k+2R-S)\,f(1).$$

Similarly, it follows from the boundedness of the solution $g(v)$ to the angular equation (32) that the solution satisfies the boundary conditions

$$(2k+1)\,g'(1)+(k-S)\,g(1)=0 \quad \text{and} \quad -(2k+1)\,g'(-1)+(k-S)\,g(-1)=0.$$

We are looking for the eigenvalues (S,E), with the smallest value of E, of the 2EP consisting of differential equations (31), (32) along with the boundedness conditions at the singular points and the boundary condition (33).

Numerical experiments show that if the scaling parameter b in the LC is carefully chosen and 60 collocation points are used for each equation, then the first four energy states for $0.1\le R\le 6$ are computed to at least 8 accurate digits. For fast convergence it is best to choose the scaling parameter b so that there are just few points on the interval where f is already very close to zero. Based on numerical experiments, we take $b=1$ for $0.1\le R\le 2$ and $b=2$ for $2<R\le 6$. By doing so we can compute the values that are given in [33, Table I and II] more accurately. In Table 4 and Table 5 we give some of the obtained values for comparison. The remaining values can be computed using function demo_hydrogen in MultiParEig. We remark that our method computes as well some solutions, that are not given in [33], for instance state $2p_u^+$ for $R=0.51$ and $R=0.515$, and state $2s_g^+$ for $R=4.5$.

Example 5. In the final numerical example we show that the ChC and multiparameter approach can be applied to 3EPs as well. As an example we consider the ellipsoidal wave equation from [45], where few first eigenmodes are computed with a technique from [4]. Although the ellipsoidal wave equation is

Table 4: Some of the values in [33, Table I], computed as solutions of a 2EP obtained by discretizing (31) by the ChC and (32) by the LC using 60 collocation points. We give separation constant S and electronic energy E_{ele} for the states $1s_g^+$ and $2p_u^+$ for some values of the internuclear separation R.

	ChC, LC, and Algorithm 2				Patil [33]			
	$1s_g^+$		$2p_u^+$		$1s_g^+$		$2p_u^+$	
R	S	E_{ele}	S	E_{ele}	S	E_{ele}	S	E_{ele}
0.100	0.018189	−7.292184	1.001124	−0.899094	0.0182	−7.2907	1.0011	−0.89912
0.200	0.064128	−6.465032	1.004661	−0.932840	0.06413	−6.4644	1.0046	−0.93288
0.300	0.128169	−5.790661	1.011210	−0.997805	0.12817	−5.7903	1.0112	−0.99782
0.500	0.290025	−4.821577	1.038783	−1.247118	0.2900	−4.8213	1.0388	−1.2471
0.510	0.298960	−4.783079	1.040867	−1.263403	–	–	–	–
0.515	0.303451	−4.764118	1.041938	−1.271642	–	–	–	–
0.800	0.579956	−3.930420	1.138223	−1.758159	0.5800	−3.9303	1.1382	−1.7581
1.000	0.789826	−3.543667	1.244195	−2.015024	0.7898	−3.5436	1.2442	−2.0150
1.500	1.337146	−2.948555	1.601105	−2.310163	1.3371	−2.9485	1.6011	−2.3101
4.000	3.972288	−2.255505	3.979869	−2.248279	3.9723	−2.2555	3.9799	−2.2483
5.000	4.980298	−2.201467	4.981731	−2.200367	4.9803	−2.2015	4.9817	−2.20037

Table 5: Some of the values in [33, Table II], computed as solutions of a 2EP obtained by discretizing (31) by the ChC and (32) by the LC using 60 collocation points. We give separation constant S and electronic energy E_{ele} for the states $2s_g^+$ and $2p_u^-$ for some values of the internuclear separation R.

	ChC, LC, and Algorithm 2				Patil [33]			
	$2s_g^+$		$2p_u^-$		$2s_g^+$		$2p_u^-$	
R	S	E_{ele}	S	E_{ele}	S	E_{ele}	S	E_{ele}
0.100	0.002149	−0.859671	1.003326	−0.886960	0.00215	−0.85965	1.0033	−0.88692
0.200	0.008198	−0.820676	1.013221	−0.881535	0.0082	−0.8207	1.0132	−0.88150
0.300	0.017614	−0.784572	1.029462	−0.873304	0.01765	−0.7846	1.0295	−0.87327
0.500	0.044999	−0.724076	1.079702	−0.851102	0.0450	−0.7241	1.0797	−0.85108
1.000	0.152031	−0.620134	1.292297	−0.782689	0.1521	−0.6201	1.2924	−0.7826
1.500	0.298946	−0.552898	1.598730	−0.715761	0.2989	−0.5529	1.5987	−0.71575
4.500	1.508425	−0.382792	4.375701	−0.471532	–	–	–	–

considered to be a very difficult computational problem, the multiparameter approach based on the ChC is quite easy to apply and gives accurate results.

We are interested in the smallest eigenfrequencies of a tri-axial ellipsoid with center $(0,0,0)$ and semi-axes $z_0 > y_0 > x_0$. In ellipsoidal coordinates (see, e.g., [4], [46, Sect. 16]), the solution of the Helmholtz equation $\nabla^2 u + \omega^2 u = 0$ is $u = X_1(\xi_1)X_2(\xi_2)X_3(\xi_3)$, where $z_0 > \xi_1 > a > \xi_2 > b > \xi_3 > 0$ for $a = (z_0^2 - x_0^2)^{1/2}$ and $b = (z_0^2 - y_0^2)^{1/2}$. After the substitution $t_i = \xi^2/b^2$ we obtain a system of second order differential equations such that all three equations for $i = 1,2,3$ have the same form

$$t_i(t_i-1)(t_i-c)X_i''(t_i) + \tfrac{1}{2}(3t_i^2 - 2(1+c)t_i + c)X_i'(t_i) + (\lambda + \mu t_i + \eta t_i^2)X_i(t_i) = 0, \tag{34}$$

where $c = a^2/b^2$, $\omega^2 = 4\eta/b^2$, and λ, μ are separation constants. The equation (34) has removable singularities at $t_i = 0$, $t_i = 1$, and $t_i = c$. It is possible to write the solution of (34) in the general form

$$X_i(t_i) = t_i^{\rho/2}(t_i-1)^{\sigma/2}(t_i-c)^{\tau/2}F_i(t_i), \tag{35}$$

where ρ, σ, and τ are either 0 or 1 (see, e.g., [4]). This gives eight possible combinations. By inserting (35) into (34) we get the final system of differential equations, where all three equations for $i = 1,2,3$

have the form

$$t_i(t_i-1)(t_i-c)F_i''(t_i)+\tfrac{1}{2}(A_2t_i^2-2A_1t_i+A_0)F_i'(t_i)+(\lambda-\lambda_0+(\mu+\mu_0)t_i+\eta t_i^2)F_i(t_i)=0, \quad (36)$$

where $\lambda_0=((\rho+\tau)^2+(\rho+\sigma)^2c)/4$, $\mu_0=(\rho+\sigma+\tau)(\rho+\sigma+\tau+1)/4$, $A_0=(2\rho+1)c$, $A_1=(1+\rho)/1+c)+\tau+\sigma c$, and $A_2=2(\rho+\sigma+\tau)+3$. We are looking for the particular solutions characterized by boundary conditions or finiteness properties [4]. When we insert $t_i=0$, $t_i=1$, and $t_i=c$ in (36), we see that the boundedness conditions at singular points lead to the following boundary conditions that involve eigenvalue parameters:

$$\begin{aligned} A_0F_3'(0)+2(\lambda-\lambda_0)F_3(0)&=0,\\ (A_2-2A_1+A_0)F_k'(1)+2(\lambda-\lambda_0+\mu+\mu_0+\eta)F_k(1)&=0 \quad \text{for} \quad k=2,3,\\ (A_2c^2-A_1c+A_0)F_k'(c)+2(\lambda-\lambda_0+(\mu+\mu_0)c+\eta c^2)F_k(c)&=0 \quad \text{for} \quad k=1,2. \end{aligned}$$

The boundedness conditions at singular points $t_i=0$, $t_i=1$, and $t_i=c$ are behavioral and the above conditions automatically appear as equations when the ChC is applied. Finally, in order to obtain a 3EP we impose the Dirichlet condition on the boundary of the ellipsoid, which gives the boundary condition

$$F_1(z_0^2/b^2)=0. \quad (37)$$

Thus we solve the 3EP which consists of the differential equations (36) together with the boundedness conditions at the singular points and the boundary condition (37).

For each of the eight possible combinations of (ρ,σ,τ) we applied the ChC on $n=20$ nodes on each of the three equations (36) to obtain an algebraic 3EP, and then computed the five eigenvalues (λ,μ,η) with the smallest $|\gamma|$ using implicitly restarted Arnoldi on $\Delta_3 w=\eta\,\Delta_0 w$. As the Δ-matrices are of size $n^3\times n^3$ and we are not aware of a method that can compute the product $\Delta_3^{-1}\Delta_0 w$ efficiently such as the Sylvester approach for 2EPs, we cannot afford so many collocation nodes as for 2EPs. If a computation with higher number of nodes is required, then a three-parameter generalization of the Jacobi–Davidson method could be applied.

From the results for all combinations of (ρ,σ,τ) we can gather the first 15 eigenmodes in Table 6. Based on the results obtained with 10, 15, and 25 collocation points, we strongly believe that the 15 smallest eigenfrequencies are computed to at least eight accurate decimals. The results agree with the first six eigenmodes that are given in [45] with four decimals. We give the plots of the corresponding wave functions in Figure 5. Smallest eigenfrequencies of an ellipsoid with different semi-axes for a given choice of (σ,ρ,τ) can be computed with function ellipsoid_eigs in MultiParEig.

8. Conclusions

We have presented a combination of spectral collocation and fast numerical methods for algebraic 2EPs. Teaming up, they can efficiently and accurately solve many 2EPs that arise when separation of variables is applied to boundary value problems, a similar idea can be applied to 3EPs. In numerical examples we show that the approach is superior to those reported in the literature; one can efficiently compute several hundreds of eigenfrequencies and the corresponding eigenmodes. Our numerical results are stable in the sense that the outcomes remain very close when we enlarge the number of collocation points N or change the scaling parameter b inside some specified ranges.

MATLAB toolbox MultiParEig with the implementations of the presented numerical methods and numerical examples provides a simple way to apply the approach on similar 2EPs and 3EPs.

It remains a challenge for the future to derive efficient methods of a Sylvester–Arnoldi type for MEPs with three or more parameters.

Table 6: First 15 eigenfrequencies for the Helmholtz equation on tri-axial ellipsoid with semi-axes $x_0 = 1$, $y_0 = 1.5$, and $z_0 = 2$. For each frequency ω we give the corresponding eigenvalue (λ, μ, η) of 3EP (36) and the combination of parameters ρ, σ, τ.

ω	λ	μ	η	ρ	σ	τ
2.34458979	0.84989209	−3.75231782	2.40498182	0	0	0
2.94367435	3.60037607	−7.76944731	3.79103317	1	0	0
3.20795093	1.48438625	−7.85091477	4.50229027	0	1	0
3.57728277	7.22643744	−13.03122756	5.59866649	0	0	0
3.78641651	5.48731495	−13.25884129	6.27241562	1	1	0
3.82663626	1.51189406	−8.87177115	6.40637596	0	0	1
4.13064732	2.05458475	−13.46994828	7.46473320	0	0	0
4.23215871	11.78829702	−19.58689645	7.83613571	1	0	0
4.38693776	5.55331827	−14.80242372	8.41978504	1	0	1
4.38859178	10.42065341	−19.87490930	8.42613530	0	1	0
4.61577934	2.12453633	−14.64930491	9.32112078	0	1	1
4.70777812	7.16950299	−20.33054607	9.69638899	1	0	0
4.89789931	17.34182024	−27.45418645	10.49537020	0	0	0
4.97229441	10.39362762	−21.87997310	10.81662385	0	0	1
5.00681461	16.33511125	−27.73496852	10.96733426	1	1	0

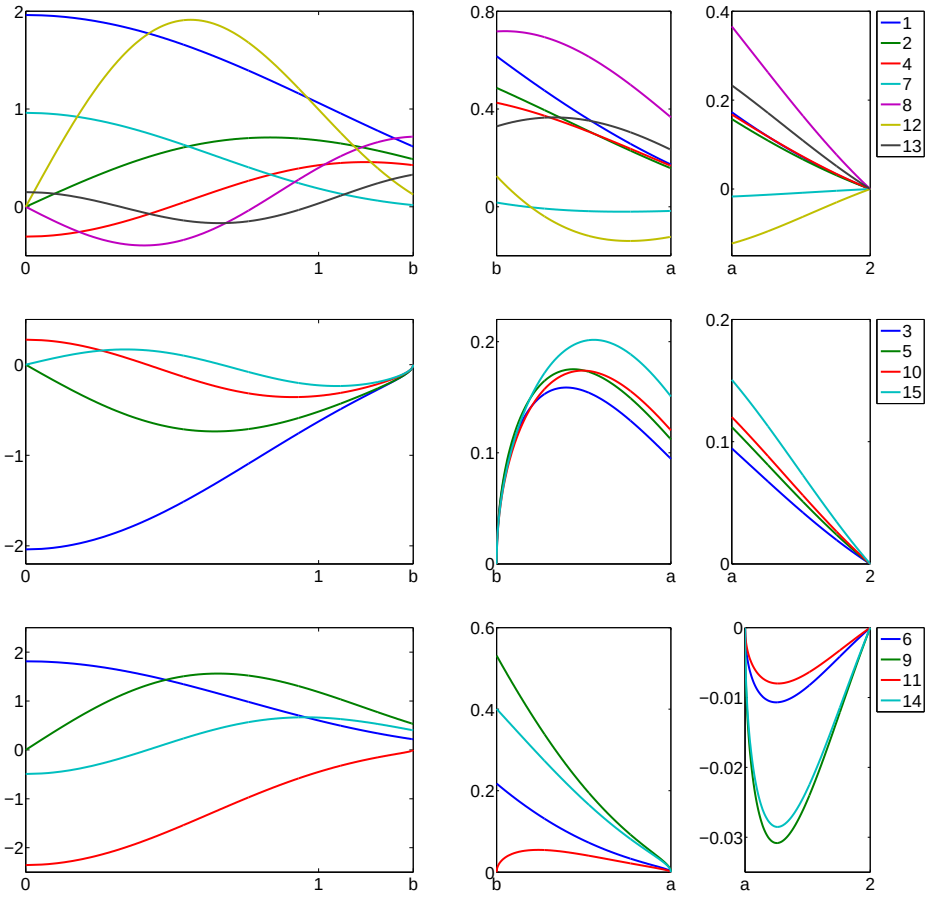

Figure 5: Plots of ellipsoidal wave functions $X_3(\xi_3)$ (left column), $X_2(\xi_2)$ (middle column), and $X_1(\xi_1)$ (right column) for the first 15 eigenmodes in Table 6. For all eigenmodes in the top row $\sigma = \tau = 0$, for all eigenmodes in the middle row $\sigma = 1$, and for all eigenmodes in the bottom row $\tau = 1$. Numbers in the legends are the indices of the eigenmodes.

Acknowledgements

We thank Guido Janssen (TU Eindhoven) for useful pointers, Joost Rommes (Mentor Graphics) for fruitful comments on the manuscript, and Miran Černe (University of Ljubljana) for helpful discussions. The research was performed in part while the first author was visiting the CASA group at the TU Eindhoven. The author wishes to thank NWO for the visitor's grant and the CASA group for its hospitality.

The authors are grateful to the referees for their careful reading and suggestions for improvement.

[1] A. A. Abramov, A. L. Dyshko, N. B. Konyukhova, and T. V. Levitina, Computation of angular wave functions of Lamé by means of solution of auxiliary differential equations, Comput. Math. Math. Phys. 29 (1989) 119–131.

[2] A. A. Abramov and V. I. Ul'yanova, A method for solving self-adjoint multiparameter spectral problems for weakly coupled sets of ordinary differential equations, Comput. Math. Math. Phys. 37 (1997) 552–557.

[3] P. Amodio, T. Levitina, G. Settani, and E. B. Weinmüller, Numerical simulation of the whispering gallery modes in prolate spheriods, Comput. Phys. Commun. 185 (2014) 1200–1206.

[4] F. M. Arscott, P. J. Taylor, and R. V. M. Zahar, On the numerical construction of ellipsoidal wave functions, Math. Comp. 40 (1983) 367–380.

[5] F. V. Atkinson, *Multiparameter Eigenvalue Problems*, Academic Press, New York, 1972.

[6] F. V. Atkinson and A. B. Mingarelli, *Multiparameter Eigenvalue Problems. Sturm–Liouville Theory*, CRC Press, Boca Raton, 2010.

[7] P. B. Bailey, The automatic solution of two-parameter Sturm-Liouville eigenvalue problems in ordinary differential equations, Appl. Math. Comput. 8 (1981) 251–259.

[8] R. H. Bartels and G. W. Stewart, Algorithm 432: Solution of matrix equation $AX + XB = C$, Comm. ACM 15 (1972) 820–826.

[9] J. Boersma and J. K. M. Jansen, Electromagnetic field singularities at the tip of an elliptic cone, EUT Report 90-WSK-Ol, TU Eindhoven, 1991.

[10] J. P. Boyd, *Chebyshev and Fourier Spectral Methods*, 2nd ed., Dover Publications, Mineola, 2001.

[11] J. P. Boyd, Chebyshev spectral methods and the Lane-Emden problem, Numer. Math. Theor. Meth. Appl. 4 (2011) 142–157.

[12] M. Faierman, *Two-parameter Eigenvalue Problems in Ordinary Differential Equations*, volume 205 of Pitman Research Notes in Mathematics Series, Longman Scientific and Technical, Harlow, 1991.

[13] B. Fornberg, *A Practical Guide to Pseudospectral Methods*, Cambridge University Press, Cambridge, 1998.

[14] C. I. Gheorghiu, *Spectral Methods for Differential Problems*, Casa Cartii de Stiinta, Cluj-Napoca, 2007.

[15] C. I. Gheorghiu, *Spectral Methods for Non-Standard Eigenvalue Problems. Fluid and Structural Mechanics and Beyond*, Springer, Cham, Heidelberg, New York, Dordrecht, London, 2014.

[16] C. I. Gheorghiu, M. E. Hochstenbach, B. Plestenjak, and J. Rommes, Spectral collocation solutions to multiparameter Mathieu's system, Appl. Math. Comp. 218 (2012) 11990–12000.

[17] G. H. Golub and C. F. Van Loan, *Matrix Computations*, 3rd ed., The Johns Hopkins University Press, Baltimore, 1996.

[18] D. Gottlieb, and S. A. Orszag, Numerical Analysis of Spectral Methods: Theory and Applications, SIAM, Philadelphia, 1977.

[19] M. E. Hochstenbach, T. Košir, and B. Plestenjak. A Jacobi–Davidson type method for the nonsingular two-parameter eigenvalue problem, SIAM J. Matrix Anal. Appl. 26 (2005) 477–497.

[20] M. E. Hochstenbach and B. Plestenjak, Harmonic Rayleigh-Ritz for the multiparameter eigenvalue problem, Elec. Trans. Numer. Anal. 29 (2008) 81–96.

[21] J. Hoepffner, Implementation of boundary conditions, `www.fukagata.mech.keio.ac.jp/~jerome/` (2007).

[22] X. Ji, On 2D bisection method for double eigenvalue problems, J. Comp. Phys. 126 (1996) 91–98.

[23] E. D. Kalinin, Modification of a method for solving the multiparameter eigenvalue problem for systems of loosely coupled ordinary differential equations, Comput. Math. Math. Phys. 53 (2013) 874–881.

[24] L. Kraus and L. Levine, Diffraction by an elliptic cone, Commun. Pure Appl. Math. 9 (1961), 49–68.

[25] J. R. Kuttler and V. G. Sigillito, Eigenvalues of the Laplacian in two dimensions, SIAM Rev. 26 (1984) 163–193.

[26] T. V. Levitina, On numerical solution of multiparameter Sturm-Liouville spectral problems. Numerical analysis and mathematical modelling, Banach Center Publ., 29, Polish Acad. Sci., Warsaw, 1994, 275–281.

[27] T. V. Levitina, A numerical solution to some three-parameter spectral problems, Comput. Math. Math. Phys. 39 (1999) 1715–1729.

[28] L. C. Lew Yan Voon and M. Willatzen, Helmholtz equation in parabolic rotational coordinates: application to wave problems in quantum mechanics and acoustics, Math. Comp. Simul. 65 (2004) 337–349.

[29] K. Meerbergen and B. Plestenjak, A Sylvester–Arnoldi type method for the generalized eigenvalue problem with two-by-two operator determinants, Report TW 653, Department of Computer Science, KU Leuven, 2014, to appear in Numer. Linear Algebra Appl.

[30] P. Moon and D. E. Spencer, *Field Theory Handbook*, Springer-Verlag, New York, 1971.

[31] J. A. Morrison, J. A. Lewis, Charge singularity at the corner of a flat plate, SIAM J. Appl. Math. 31 (1976) 233–250.

[32] F. W. J. Olver (Ed.), *NIST Handbook of Mathematical Functions*, Cambridge University Press, Cambridge, 2010.

[33] S. H. Patil, Hydrogen molecular ion and molecule in two dimensions, J. Chem. Phys. 118 (2003) 2197–2205.

[34] B. Plestenjak, A continuation method for a right definite two-parameter eigenvalue problem, SIAM J. Matrix Anal. Appl. 21 (2000) 1163–1184.

[35] B. Plestenjak, MultiParEig, `www.mathworks.com/matlabcentral/fileexchange/47844-multipareig`, MATLAB Central File Exchange. Retrieved September 14, 2014.

[36] B. D. Sleeman, Multiparameter spectral theory and separation of variables, J. Phys. A: Math. Theor. 41 (2008) 1–20.

[37] D. C. Sorensen, Implicit application of polynomial filters in a k-step Arnoldi method, SIAM J. Matrix Anal. Appl. 13 (1992) 357–385.

[38] G. W. Stewart, A Krylov–Schur algorithm for large eigenproblems, SIAM J. Matrix Anal. Appl., 23 (2001), 601–614.

[39] T. Toolan, lapack, `www.mathworks.com/matlabcentral/fileexchange/16777-lapack`, MATLAB Central File Exchange. Retrieved August 20, 2014.

[40] L. N. Trefethen, *Spectral Methods in MATLAB*, SIAM, Philadelphia, 2000.

[41] H. Volkmer, *Multiparameter Problems and Expansion Theorems*, Lecture Notes in Math. 1356, Springer-Verlag, New York, 1988.

[42] J. A. C. Weideman, DMSUITE, `www.mathworks.com/matlabcentral/fileexchange/29-dmsuite`, MATLAB Central File Exchange. Retrieved August 20, 2014.

[43] J. A. C. Weideman and S. C. Reddy, A MATLAB differentiation matrix suite, ACM Trans. Math. Softw. 26 (2000) 465–519.

[44] M. Willatzen and L. C. Lew Yan Voon, Theory of acoustic eigenmodes in parabolic cylindrical enclosures, J. Sound Vib. 286 (2005) 251–264.

[45] M. Willatzen and L. C. Lew Yan Voon, Numerical implementation of the ellipsoidal wave equation and application to ellipsoidal quantum dots, Comput. Phys. Commun. 171 (2005) 1–18.

[46] M. Willatzen and L. C. Lew Yan Voon, *Separable Boundary-Value Problems in Physics*, Wiley-VCH, Weinheim, 2011.

Appendix A. MATLAB package

The methods and examples presented in this paper are part of the package MultiParEig, which is freely available on MATLAB Central File Exchange [35]. It requires package DMSUITE [42], which has to be installed. For a better performance we suggest to install package LAPACK [39] as well.

We give a short overview of functions in the package that are related to the paper, for details see the built-in help and the attached examples.

- [lambda,mu,X1,X2] = twopareig(A1,B1,C1,A2,B2,C2) solves a 2EP using Algorithm 1. For a 3EP, use [lambda,mu,eta,X1,X2,X3] = threepareig(A1,B1,C1,D1,...,A3,B3,C3,D3), which uses a generalization of Algorithm 1.

- [lambda,mu,X1,X2] = twopareigs(A1,B1,C1,A2,B2,C2,k) returns k eigenvalues of a 2EP with the smallest $|\mu|$ using the implicitly restarted Arnoldi variant of Algorithm 2. The Krylov–Schur variant is implemented in twopareigs_ks, which has the same syntax. See also threepareigs, which computes k eigenvalues of a 3EP with the smallest $|\eta|$.

- [z,A,B,C,G,k,r] = bde2mep(a,b,p,q,r,s,t,bc,N) discretizes boundary value equation (13) with the ChC using N points. Functions p,q,r,s, and t should be either scalar MATLAB functions or constants. Boundary conditions $\alpha y(a)+\beta y'(a)=0$ and $\gamma y(b)+\delta y'(b)=0$ are given in matrix bc=[alpha beta; gamma delta]. The function returns matrices A,B,C of size $(N-2)\times(N-2)$, vector of collocation nodes z, give-back matrix G, and sets of kept indices k and removed indices r. From G, k, and r the solution in all collocation nodes can be reconstructed by function recover_bc. See also bde3mep with a similar syntax for 3EPs.

- [omega,G,F,eta,xi] = ellipse_eigs(mode,alpha,beta,m,n) returns the first m even (mode=1) or odd (mode=2) eigenfrequencies and eigenmodes of an elliptical membrane with major and minor axis alpha and beta, where Mathieu's system (1) is discretized by the ChC with n=[n1 n2] points for the first and the second equation. See ellipsoid_eigs for the first m eigenfrequencies and eigenmodes of an ellipsoid with semi-axes $x_0<y_0<z_0$.

From the following examples one can learn how to solve a given 2EP or 3EP (to run the examples, MultiParEig should be in the MATLAB path):

- demo_besselwave1 solves the Bessel wave equations (24)–(25) and computes the values in Table 2. See also demo_besselwave_figs, which plots Figure 2, demo_besselwave2, which plots Figure 3 ([28, Fig. 5]), and demo_besselwave3, which reconstructs [28, Figs. 6a, 6b, and 6c].

- demo_ellipsoidwave computes eigenmodes for the ellipsoid wave equation (34) in Table 6. See also demo_ellipsoidwave_figs that plots the wave functions in Figure 5.

- demo_hydrogen computes states of hydrogen molecular ion in 2D from the 2EP (31)–(32) and gives the values in Tables 4 and 5.

- demo_lame gives the eigenvalues for Lame's system (22)–(23) in Table 1. See also demo_lame_conv, which plots Figure 1.

- demo_mathieu solves Mathieu's system (1), gives the first 300 even eigenfrequencies for an elliptical membrane with axis $\alpha=2$ and $\beta=1$, and plots eigenmodes no. 298 and 300 ([16, Figs. 5 and 6]).

- demo_weber computes eigenvalues for the Weber equations (28)–(29) in Table 3 and plots the eigenmodes. See also demo_weber_figs, which plots Figure 4.